

# Convergent close-coupling calculations of positron scattering from carbon

Nicolas A. Mori\*, Liam H. Scarlett, Igor Bray and D.V. Fursa

Curtin University, Perth, Western Australia

\*[nicolas.mori@postgrad.curtin.edu.au](mailto:nicolas.mori@postgrad.curtin.edu.au)

December 14, 2022



# Introduction: Motivation

Introduction

Method

Results

Conclusion

Acknowledgements

- Positrons are important in medical industry - positron emission tomography (PET) and positron therapy.
- Quantifiable data of scattering processes occurring in these technologies scarce and largely unknown.
- Many modern scattering methods require accurate cross sections for each constituent atom to model the interactions occurring with positrons and biomolecules in these cases.
- Positronium-formation important, in particular, as its decay results in 80 % of detected gamma rays in PET scans.
- With this data can increase accuracy of PET scans and model positron therapy.

# Introduction: CCC-method

Introduction

Method

Results

Conclusion

Acknowledgements

- Have extended atomic single-center convergent close-coupling (CCC) to calculate scattering from multi-electron atoms, without requirement of frozen-core.
- Achieved through utilisation of Multiconfigurational Hartree-Fock (MCHF) method of Fischer [*Comp. Phys. Comm.* 64, 369 (1991)] and MULT codes of Zatsarinny [*Comp. Phys. Comm.* 174, 273 (2006)]
- Have calculated comprehensive scattering data for positron scattering from carbon.
- Addressed deficits in single-center method through use of complex model potential.

# Method: Atomic structure calculation

Introduction

Method

Results

Conclusion

Acknowledgements

- Target Hamiltonian:

$$H_T = \sum_{i=1}^{N_e} \left( -\frac{1}{2} \nabla_i^2 - \frac{Z}{r_i} \right) + \sum_{i>j=1}^{N_e} \frac{1}{|r_i - r_j|}$$

- Configuration-interaction representation of wave function:

$$\Phi_n^N(x_1, \dots, x_{N_e}) = \sum_{i=1}^N C_i^{(n)} \phi_i(x_1, \dots, x_{N_e})$$

- Radial functions obtained via MCHF calculation or Laguerre basis functions:

$$\begin{aligned} \varphi_{k\ell}(r) &= \sqrt{\frac{\alpha_\ell (k-1)!}{(k+\ell)(k+2\ell)!}} (2\alpha_\ell r)^{\ell+1} \\ &\times e^{-\alpha_\ell r} L_{k-1}^{2\ell+1}(2\alpha_\ell r), \quad k = 1, \dots, N_\ell. \end{aligned} \quad (1)$$

- Diagonalize target Hamiltonian to obtain CI coefficients.
- Pseudostates satisfy:  $\langle \Phi_n^N | H_T | \Phi_m^N \rangle = \epsilon_n^N \delta_{nm}$

# Method: Single-Center Convergent Close-Coupling

Introduction

Method

Results

Conclusion

Acknowledgements

- Total scattering Hamiltonian:  $H = H_T - \frac{1}{2}\nabla_0^2 + V$
- Schrödinger equation for total scattering wave function:  $(H - E)|\Psi_i^{(+)}\rangle = 0$
- Solve through expanding wavefunction in set of target pseudostates:

$$\Psi_i^{N(+)} = \sum_{n=1}^N F_n^{N(+)}(\mathbf{r}_0) \Phi_n^N(\hat{\mathbf{r}}_1, \dots, \hat{\mathbf{r}}_N)$$

- Coupled Lippman-Schwinger equations for the  $T$  matrix:

$$\begin{aligned} \langle \mathbf{k}_f \Phi_f^N | T | \Phi_i^N \mathbf{k}_i \rangle &= \langle \mathbf{k}_f \Phi_f^N | V | \Phi_i^N \mathbf{k}_i \rangle \\ &+ \sum_{n=1}^N \int d\mathbf{k} \frac{\langle \mathbf{k}_f \Phi_f^N | V | \Phi_n^N \mathbf{k} \rangle \langle \mathbf{k} \Phi_n^N | T | \Phi_i^N \mathbf{k}_i \rangle}{E^{(+)} - \epsilon_n^N - \epsilon_k} \end{aligned}$$

- Perform partial-wave expansion of the projectile plane waves and solve the Lippmann-Schwinger equations per total scattering-system angular momentum  $J$ .

# Method: Single-Center Convergent Close-Coupling Drawbacks

Introduction

Method

Results

Conclusion

Acknowledgements

- Approach unstable between positronium-formation threshold and ionization threshold.
- Occurs because boundary conditions with channels corresponding to positive-energy pseudostates are closed while positronium-formation channels are open.
- Positronium-formation included implicitly therefore cannot separate positronium-formation and direct ionization.

# Method: CCC-scaled Complex Model Potential

Introduction

Method

Results

Conclusion

Acknowledgements

- Complex potential:  $V_{\text{opt}}(r, E_i) = V_{\text{st}}(r) + V_{\text{pol}}(r) + iV_{\text{abs}}(r, E_i)$
- Static potential:  
$$V_{\text{st}}(r) = \frac{Z}{r} - 4\pi \left( \frac{1}{r} \int_0^r dr' \rho(r') r'^2 + \int_0^\infty dr' \rho(r') r' \right)$$
- Polarization potential:  $V_{\text{pol}}(r) = -\frac{\alpha_D}{2(r^2+d^2)^2}$
- Absorption potential:

$$V_{\text{abs}}(r, E_i) = -\rho(r) \left[ \sqrt{\frac{T_{\text{loc}}}{2}} \left( \frac{8\pi}{10k_F^3(r)E_i} \right) \times \theta(k_i^2 - k_F^2(r) - 2\Delta)(A_1 + A_2 + A_3) \right]$$

- Staszewska *et al.* [*J. Chem. Phys.* 81, 335 (1984)].
- Absorption threshold:  $\Delta(E) = \Delta_e - (\Delta_e - \Delta_p)e^{-(E_i - \Delta_p)/E_m}$
- Form from Chiari *et al.* [*J. Phys. B: At Mol Opt* 45, 215206 (2012)]

# Method: CCC-scaled Complex Model Potential

Introduction

Method

Results

Conclusion

Acknowledgements

- Solve Lippman-Schwinger equation:

$$\langle \mathbf{k}_f | T | \mathbf{k}_i \rangle = \langle \mathbf{k}_f | V | \mathbf{k}_i \rangle + \int d\mathbf{k} \frac{\langle \mathbf{k}_f | V | \mathbf{k} \rangle \langle \mathbf{k} | T | \mathbf{k}_i \rangle}{k_i^2/2 - k^2/2 + i0}$$

- Obtain partial-wave Lippman-Schwinger equation:

$$T_\ell(k_f, k_i) = V_\ell(k_f, k_i) + \mathcal{P} \int_0^\infty dk \frac{V_\ell(k_f, k) T_\ell(k, k_i)}{k_i^2/2 - k^2/2} - \frac{i\pi}{k_i} V_\ell(k_i, k_i) T_\ell(k_i, k_i)$$

- Total cross section:  $\sigma_{\text{tot}} = 4\pi^3 \sum_{l=0}^\infty (2l+1) |T_l|^2$
- Elastic cross section:  $\sigma_{\text{el}} = -\frac{4\pi^2}{\sqrt{2E_i}} \sum_{\ell=0}^\infty (2\ell+1) \text{Im}(T_\ell)$
- Calculate positronium-formation with delta-variational technique.
- Scale direct inelastic component to agree at high energy limit with single-center CCC.
- Scale positronium-formation component to agree at the maximum cross section between ionization threshold and 10 eV above it.



# Calculation Details

Introduction

Method

Results

Conclusion

Acknowledgements

- A MCHF calculation for  $C^+$  was used to obtain orbitals  $1s$  to  $5s$ .
- All other orbitals obtained by Laguerre basis with  $N_\ell = 18 - \ell$ ,  $\ell_{max} = 8$ , and  $\alpha_\ell = 1.0$ .
- Configurations included:  $2s^2 2pn\ell$  continuum for  $\ell \leq 8$ ,  $2s 2p^2 n\ell$  for  $\ell \leq 4$ ,  $2p^3 n\ell$  for  $\ell \leq 2$ ,  $2s 2pn\ell' n\ell$  and  $2s 2pn\ell^2$  for  $n\ell$  and  $n'\ell'$  between  $3s$  and  $5s$ .
- Included target states with excitation energies 40 eV above ionization threshold, resulting in 943 target states.
- Calculations completed to  $J = 10$  partial waves.
- Extrapolated ionization cross section at high energies with a 4571-state Born calculation.

# Convergence study

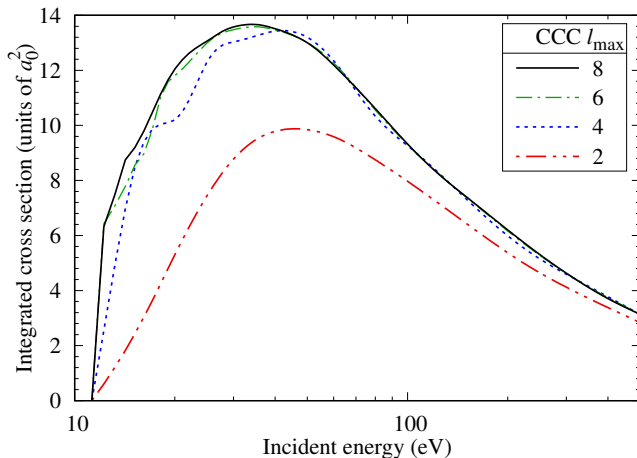
Introduction

Method

Results

Conclusion

Acknowledgements



- Convergence study of total ionization cross section for  $l_{\max} = 2$  to  $l_{\max} = 8$ .
- Convergence established for  $l_{\max} > 6$  for energies above 15 eV.

# Results: Structure

Introduction

Method

Results

Conclusion

Acknowledgements

## ● Excitation energies and oscillator strength for carbon

	State	Term	CCC	Ref. [1]	Ref. [2]	Ref. [3]	NIST. [4]
1	$2s^2 2p^2$	$^3P$	0.000	0.000	0.000	0.000	0.000
2	$2s^2 2p^2$	$^1D$	1.372	1.302	1.557	1.545	1.260
3	$2s^2 2p^2$	$^1S$	2.748	2.629	2.602	2.545	2.680
4	$2s 2p^3$	$^5S^o$	3.940	3.963	3.092	3.133	4.179
5	$2s^2 2p 3s$	$^3P^o$	7.617	7.527	7.401	8.488	7.481
6	$2s^2 2p 3s$	$^1P^o$	7.818	7.750	7.740	8.936	7.680
7	$2s 2p^3$	$^3D^o$	7.951	8.004	8.340	8.412	7.942
8	$2s^2 2p 3p$	$^1P$	8.897	8.534	8.451	9.456	8.534
9	$2s^2 2p 3p$	$^3D$	9.032	8.649	8.600	9.589	8.642
10	$2s^2 2p 3p$	$^3S$	9.188	8.775	8.772	9.785	8.767
11	$2s^2 2p 3p$	$^3P$	9.332	8.857	9.309	10.390	8.845
12	$2s 2p^3$	$^3P^o$	9.481	9.379	9.517	9.981	9.326
13	$2s^2 2p 3p$	$^1D$	9.553	9.014	9.443	10.757	8.998
14	$2s^2 2p 3p$	$^1S$	9.766	9.172	10.424	11.370	9.168
15	$2s^2 2p 3d$	$^1D^o$	10.166	9.614	9.772	10.719	9.627
16	$2s^2 2p 4s$	$^3P^o$	10.258	9.673	10.142	10.810	9.683
17	$2s^2 2p 3d$	$^3F^o$	10.271	9.687	9.517	10.809	9.695
18	$2s^2 2p 3d$	$^3D^o$	10.288	9.705	9.607	10.888	9.705
19	$2s^2 2p 4s$	$^1P^o$	10.301	9.685	9.549	10.834	9.709
20	$2s^2 2p 3d$	$^1F^o$	10.333	9.716	9.607	10.947	9.732
21	$2s^2 2p 3d$	$^1P^o$	10.370	9.748	9.653	10.970	9.758
22	$2s^2 2p 3d$	$^3P^o$	10.404	9.840	13.407	11.018	9.830
lon.	Limit		11.234				11.268
23	$2s 2p^3$	$^1D^o$	13.600	12.968	14.470	14.645	
24	$2s 2p^3$	$^3S^o$	13.279	13.073	13.407	15.366	13.117
25	$2s 2p^3$	$^1P^o$	15.883	15.401	15.927	16.182	

Lower level	Upper level	CCC	Ref. [1]	Ref. [2]	Ref. [3]	NIST. [4]
$2s^2 2p^2 \ ^3P$	$2s^2 2p 3s \ ^1P^o$	0.146	0.143	0.124	0.154	0.140
	$2s 2p^3 \ ^3D^o$	0.076	0.073	0.098	0.152	0.072
	$2s 2p^3 \ ^3P^o$	0.078	0.056	0.028	0.117	0.063
	$2s^2 2p 3d \ ^3D^o$	0.037	0.027	0.023	0.010	0.021
	$2s^2 2p 3d \ ^3P^o$	0.144	0.096	0.112	0.132	0.094
	$2s^2 2p 3d \ ^3P^o$	0.037	0.037	0.340	0.069	0.040
	$2s 2p^3 \ ^3S^o$	0.143	0.156	0.171	0.269	0.152
$2s^2 2p^2 \ ^1D$	$2s^2 2p 3s \ ^1P^o$	0.118	0.103	0.128	0.103	0.118
	$2s^2 2p 3d \ ^1D^o$	0.017	0.012	0.009	0.007	0.013
	$2s^2 2p 4s \ ^1P^o$	0.015	0.007	0.004	0.010	0.011
	$2s^2 2p 3d \ ^1F^o$	0.123	0.080	0.061	0.099	0.085
	$2s^2 2p 3d \ ^1P^o$	0.011	0.011	0.018	0.014	0.009
	$2s 2p^3 \ ^1D^o$	0.256	0.224	0.344	0.529	
	$2s 2p^3 \ ^1P^o$	0.151	0.155	0.351	0.333	
$2s^2 2p^2 \ ^1S$	$2s^2 2p 3s \ ^1P^o$	0.088	0.090	0.021	0.0076	0.094
	$2s^2 2p 4s \ ^1P^o$	0.008	0.011	0.007	0.001	0.005
	$2s^2 2p 3d \ ^1P^o$	0.170	0.116	0.050	0.142	0.125
	$2s 2p^3 \ ^1P^o$	0.148	0.124	0.122	0.633	

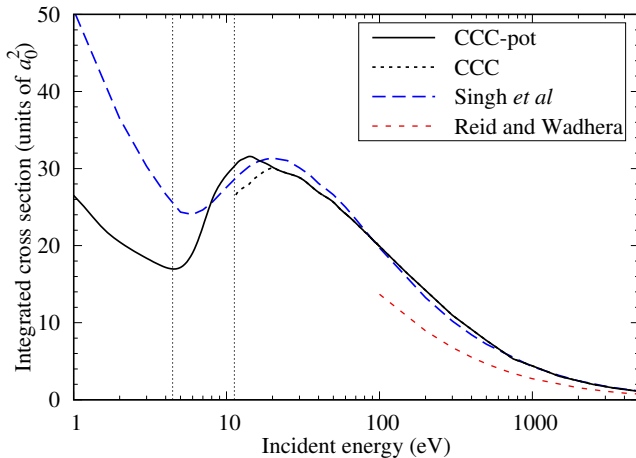
[1] Wang et al. [Phys. Rev. A 87, 012704 (2013)]

[2] Stancalie et al. [J. Phys. B: At. Mol. Opt. Phys. 576, 01201 0(2015)]

[3] Dunseath et al. [J. Phys. B: At. Mol. Opt. Phys. 30, 277 (1997)]

[4] NIST [https://www.nist.gov/]

# Results: Total Cross Section



- Agreement with Singh *et al.* [*J. Phys. Chem. A* 120, 5685 (2016)] at high energies, Reid and Wadhra [*J. Phys. B.: At. Mol. Opt. Phys* 47, 225211 (2014)] underestimate both theories.

# Results: Total Ionization Cross Section

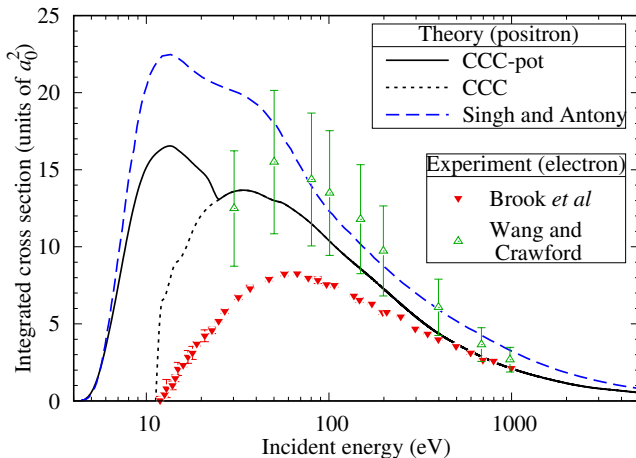
Introduction

Method

Results

Conclusion

Acknowledgements



- Results of Singh and Antony [*J. App. Phys.* 119, 50006 (2017)] higher for all energies beside threshold. Agreement viewed with electron experiment of Brook *et al.* [*J. Phys. B.: At. Mol. Opt. Phys.* 1, 3115 (1978)] above 500 eV.

# Results: Positronium-formation Cross Section

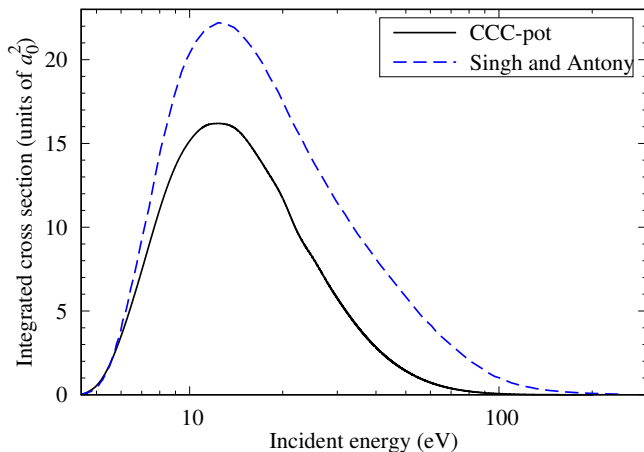
Introduction

Method

Results

Conclusion

Acknowledgements



- CCC-scaled model potential lower than Singh and Antony [*J. App. Phys.* 119, 50006 (2017)] for energies above 5 eV.

# Results: Direct Ionization Cross Section

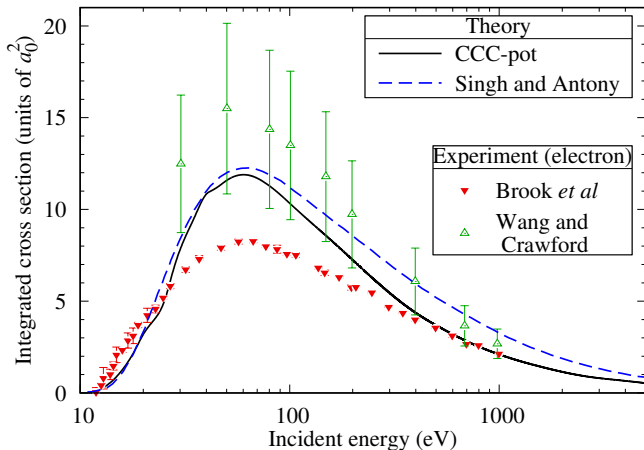
Introduction

Method

Results

Conclusion

Acknowledgements



- Singh and Antony [*J. App. Phys.* 119, 50006 (2017)] and CCC in agreement below 40 eV. Agreement between CCC and electron experiment of Brook et al. [*J. Phys. B.: At. Mol. Opt. Phys.* 1, 3115 (1978)] above 500 eV.

# Results: Elastic Cross Section

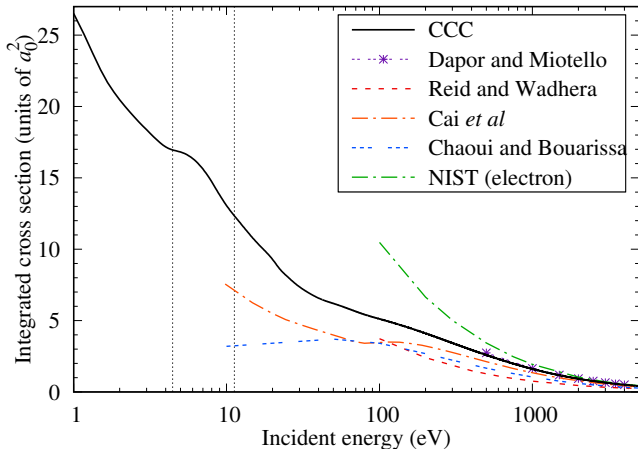
Introduction

Method

Results

Conclusion

Acknowledgements



- Close agreement with CCC and calculations of Dapor and Miotello [*At. Data and Nucl. Data Tables* 69, 1 (1998)].
- Agreement with electron NIST [<https://srdata.nist.gov/srd64/> (2016)] results above 2500 eV.



# Results: Elastic Differential Cross Section

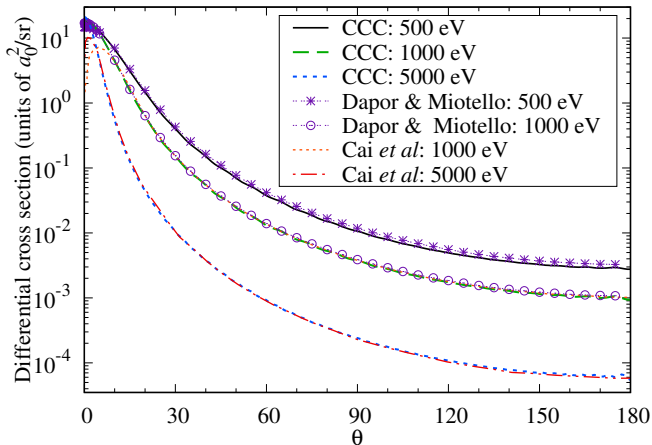
Introduction

Method

Results

Conclusion

Acknowledgements



- Close agreement between all theory, except for Cai *et al.* [*J. Phys. Conf. Ser.* 262, 012009 (2011).] at low angles.

# Results: Momentum Transfer Cross Section

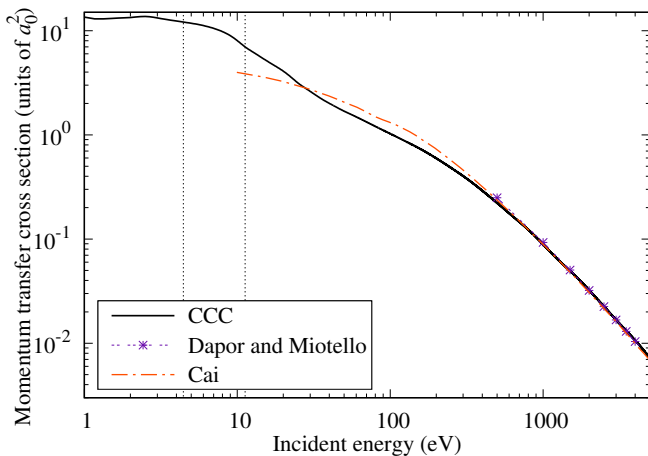
Introduction

Method

Results

Conclusion

Acknowledgements



- Close agreement between all theory above 750 eV.

# Results: Low-energy scattering

Introduction

Method

Results

Conclusion

Acknowledgements

- From low-energy results can calculate scattering length of  $-5.03 a_0$ .
- Can use this to calculate energy of positron-carbon virtual state: 0.537 eV.
- Hidden Ramsauer-Townsend minimum in elastic cross-section, can be observed in  $s$ -wave component and MTCS.
- Has been demonstrated for noble gases [ *Dzuba et al., J. Phys. B: Atom. Mol. Phys. 29, 3151 (1996).* ], [ *Green et al., Phys. Rev. A 90, 032712 (2014).* ], [ *F. Arretche, M. V. Barp, W. Tenfen, and E. P. Seidel, Braz. J. Phys 50, 844 (2020).* ] .

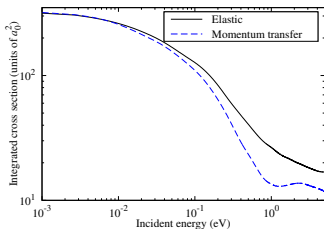


Figure: Low-energy elastic and momentum transfer cross section.

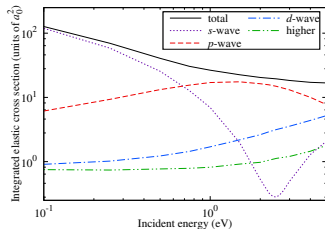
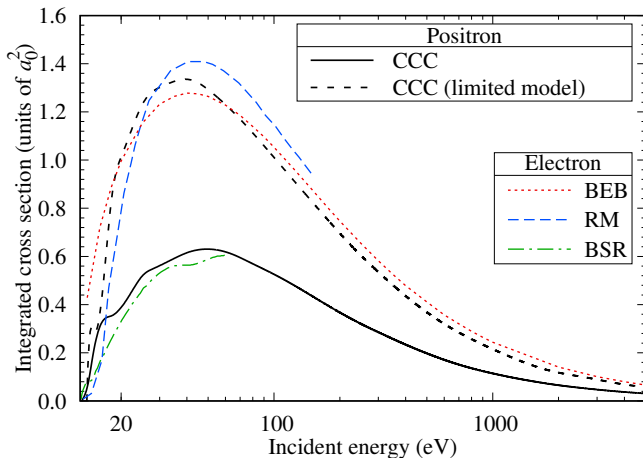


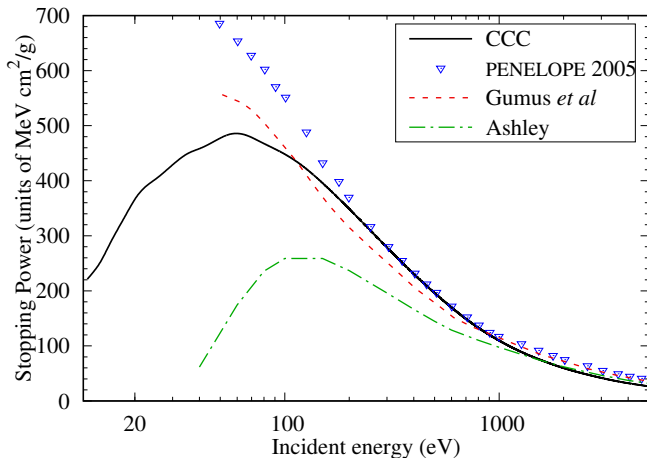
Figure:  $s$ -,  $p$ -,  $d$ - and higher wave components of elastic cross-section.

# Results: Excitation to $3S^o$



- Magnitude in closer agreement with electron-impact BSR [*Phys. Rev. A* 87, 012704 (2013)] results.
- Limited model agreement with other electron-impact calculations suggests inadequate description of  $2s2p^2nl$  continuum.

# Results: Stopping Power



- PENELOPE [*NEA Databank (2004)*] code in agreement with CCC above 250 eV.
- Ashley [*J. Electron Spectrosc. Relat. Phenom. 50, 323 (1990)*] results in agreement with CCC above 1500 eV.

# Conclusion

Introduction

Method

Results

Conclusion

Acknowledgements

- Calculated comprehensive cross section data for positron scattering on carbon for various cross sections.
- Also calculated energy of virtual state, scattering length, and stopping power.
- Agreement viewed with carbon experiment and other theory for high energies, with exception for Singh and Antony [*J. App. Phys.* 119, 50006 (2017)] results for ionization.
- Discrepancies present between previous theory at lower energies.

# Acknowledgements

Introduction

Method

Results

Conclusion

Acknowledgements

- Pawsey supercomputing centre.
- Australian government.
- AIP congress.
- Audience.